

Published in final edited form as:

Neurosci Lett. 2008 December 5; 447(1): 42–47. doi:10.1016/j.neulet.2008.09.050.

Olfactory sensory deprivation increases the number of proBDNF-immunoreactive mitral cells in the olfactory bulb of mice

K.C. Biju¹, Thomas Gerald Mast¹, and Debra Ann Fadool²

¹ Department of Biological Science, ^{1,2} Program in Neuroscience, The Florida State University, Tallahassee, FL 32306

² Molecular Biophysics, 3008, Life Science (KIN), 319 Stadium Drive, The Florida State University, Tallahassee, FL 32306

Abstract

In the olfactory bulb, apoptotic cell-death induced by sensory deprivation is restricted to interneurons in the glomerular and granule cell layers, and to a lesser extent in the external plexiform layer, whereas mitral cells do not typically undergo apoptosis. With the goal to understand whether brain-derived neurotrophic factor (BDNF) mediates mitral cell survival, we performed unilateral-naris occlusion on mice at postnatal day one (P1) and examined the subsequent BDNF immunoreactive (BDNF-ir) profile of the olfactory bulb at P20, P30, and P40. Ipsilateral to the naris occlusion, there was a significant increase in the number of BDNF-ir mitral cells per unit area that was independent of the duration of the sensory deprivation induced by occlusion. The number of BDNF-ir juxtglomerular cells per unit area, however, was clearly diminished. Western blot analysis revealed the presence of primarily pro-BDNF in the olfactory bulb. These data provide evidence for a neurotrophic role of proBDNF in the olfactory system of mice and suggest that proBDNF may act to protect mitral cells from the effects of apoptotic changes induced by odor sensory deprivation.

Keywords

TrkB; naris occlusion; neurotrophin; apoptosis; brain-derived neurotrophic factor

Introduction

Sensory activity shapes the structure and function of the developing olfactory system [4,21, 25]. When olfactory cues are deprived by unilateral-naris occlusion in neonatal rats, the olfactory bulb (OB) ipsilateral to the occlusion is ~ 25% smaller than that of the contralateral OB [5,22]. This reduction is principally attributed to apoptotic cell death of interneurons in the glomerular and granule cell layers [25]. The number of mitral cells, the major projection neuron, is unaffected by unilateral-naris occlusion [25].

Brain-derived neurotrophic factor (BDNF), a member of the neurotrophin family, regulates neuronal survival, growth, synaptic plasticity, and modulates ion channel activity [3]. TrkB,

To Whom All Correspondence Should Be Directed: Debra Ann Fadool, 3008 Life Science (KIN), 319 Stadium Drive, Programs in Neuroscience and Molecular Biophysics, Florida State University, Tallahassee FL 32306, Telephone: 850 644-4775, Facsimile: 850 645-3281, E-mail: dfadool@bio.fsu.edu.

Publisher's Disclaimer: This is a PDF file of an unedited manuscript that has been accepted for publication. As a service to our customers we are providing this early version of the manuscript. The manuscript will undergo copyediting, typesetting, and review of the resulting proof before it is published in its final citable form. Please note that during the production process errors may be discovered which could affect the content, and all legal disclaimers that apply to the journal pertain.

the preferred high-affinity receptor for BDNF, is expressed in the OB [28]. There is a time-dependent modulation of potassium current in mitral cell neurons in response to acute or chronic BDNF stimulation [28]. BDNF-activation of TrkB receptors causes phosphorylation of tyrosine residues on the *Shaker* family member, Kv1.3, which is highly expressed in mitral cells [7]. Moreover, juxtaposition of unstimulated TrkB receptors with Kv1.3 channels modulates the resident half-life of the channel in the plasma membrane [8]. Thus, BDNF modulation of mitral cell excitability is well known, while BDNF regulation of mitral cell survival is not. This study monitored the BDNF immunoreactive (ir) profile of OB neurons in order to understand the role of BDNF following sensory deprivation. Special attention was directed to mitral cells because 1) these neurons do not undergo apoptosis following unilateral-naris occlusion and 2) we know these neurons express TrkB receptors and undergo changes in excitability upon stimulation by BDNF.

Materials and methods

Solutions and antisera

Solutions used for protein samples or tissue preparation, namely, nonidet-P40 protease and phosphatase inhibitor (NP40 PPI), homogenization buffer (HB), and phosphate-buffered saline (PBS), were made as previously [28]. The BDNF antiserum was from Santa Cruz Biotechnology, (Santa Cruz, CA, cat # sc-546). BDNF antiserum recognizes both the proneurotrophin ($M_r=27$ kDa) as well as the mature neurotrophin ($M_r=13$ kDa). Monoclonal actin antiserum (cat # A-2066) was from Sigma-Aldrich (St. Louis, MO) and used at 1:1000 for Western blots. All electrophoresis reagents were from Sigma-Aldrich.

Unilateral-naris occlusion procedures

C57BL/6 mice (Jax Laboratories, Jacksonville, FL, USA) were anesthetized by hypothermia and the left naris was cauterized using a heated metal probe inserted 1–2 mm into the nostril at postnatal day one (P1) as described previously [22,28]. The animals were then warmed to 37 C and returned to the dam. Scar formation resulted in permanent unilateral-naris closure. To facilitate the study of morphological changes in mitral cells that might accompany the unilateral-naris occlusion, *thy1*-yellow fluorescent protein transgenic mice (YFP mice) [12] were handled as above. Previously, we used this mouse to identify mitral cells and their dendritic processes [20]. All procedures were carried out as approved by the Florida State University Laboratory Animal Resources and the National Institutes of Health.

At postnatal day (P) 20, 30 and 40, complete closure of the cauterized nostril was confirmed by visual examination under a dissecting microscope. Animals were perfused using paraformaldehyde dissolved in phosphate-buffered saline (4% PFA/PBS); the olfactory bulbs (OBs) were removed and post-fixed in 4% PFA/PBS for 4 hours (h). OBs were cryoprotected in 30% sucrose and 16 μm coronal sections were placed onto gelatin-coated slides, and stored at -20°C until use.

Anatomical Analysis

Avidin–biotin–peroxidase (ABC) methods were employed to localize BDNF (anti-BDNF 1:1000 dilution) in OB tissue sections as per manufacturer's protocols (ABC Elite Kit, Vector Laboratories, Burlingame, CA). Fifteen animals of each treatment condition (control = C, naris occluded = O) per occlusion duration (20, 30, or 40 days) were sampled. An investigator blind to the deprivation condition counted BDNF-ir mitral or juxtglomerular cells within 12 fields of view using 93,500 μm^2 areas and sampling equally (3 sections each) from the dorsal, ventral, medial, and lateral aspects of the OB. The counts from these 12 sampled areas were then averaged for the analysis. Statistical significance was determined at the 95% confidence level

by mixed block factorial design analysis of variance (ANOVA) with a *Bonferoni's* post-hoc test to compare the multiple factors of naris-occlusion and duration.

Confocal Microscopy

Olfactory bulb sections from YFP mice were prepared as above, except a 4°C overnight incubation with anti-BDNF was followed by 2 h incubation in Alexa Fluor 546-conjugated anti-rabbit IgG (1:100; Invitrogen, Carlsbad, CA) and a five min incubation with DAPI (1:5000). Sections were rinsed, mounted with Vectashield (Vector Laboratories, Burlingame, CA), and viewed using a Zeiss LSM510 two-photon confocal system (Thornwood, NY). Image brightness and contrast were adjusted with Adobe Photoshop CS (Adobe Systems Inc., San Jose, CA) for maximal clarity.

Biochemistry

Twenty days after unilateral-naris or sham (probe to shank of nose) occlusion, the OBs were harvested following euthanasia with CO₂. Tissues from 3 animals were pooled and homogenized in Nonidet-P40 protease and phosphatase inhibitor (NP40 PPI) buffer and detergent-soluble proteins were extracted as previously described [10]. Cytoplasmic proteins (50 µg/lane) were separated on 15% bis-acrylamide gels by SDS-PAGE and electro-transferred to nitrocellulose as previously described [10]. Membranes were blocked for 30 min with 5% nonfat milk and incubated overnight at 4°C in anti-BDNF (1:200). The nitrocellulose was then incubated with horseradish peroxidase-conjugated donkey anti-rabbit IgG (1:5000, GE Healthcare, Piscataway, NJ) for 90 min at room temperature. Enhanced chemiluminescence (GE Healthcare) exposure on Classic Blue film (Midwest Scientific; St. Louis, MO) was used to visualize labeled proteins. Paired treatments (sham, contralateral, and ipsilateral) were compared on the same film to standardize differences in exposure between films.

Results

Prior to the preparation of histological samples, animals were visually confirmed to have complete naris closure and reduced OB size ipsilateral to the naris occlusion as anticipated [22] and shown in Figure 1A. Independent of postnatal age, the OB contralateral (open) to the naris closure consistently revealed BDNF-ir in mitral cells, juxtglomerular cells, and in the fibers contained in the external plexiform layer (EPL) (Figure 1C). Strongly labeled fibers were evident along the superficial (outer) layer of the EPL (oEPL) and glomerular layer (GL) (Figure 1C). All BDNF-ir profiles were abolished when the antiserum was preadsorbed with rhBDNF (Figure 1D) or when the primary antiserum was omitted (Figure 1E). Ipsilateral to the naris occlusion, the glomeruli (data not shown) as well as the EPL were reduced in size (Figure 1B). BDNF-ir fibers in the oEPL and in the GL were markedly reduced (Figure 1B). Moreover, as early as P20 an increase in the number of BDNF-ir mitral cells per unit area (see methods) was observed (Figure 1B).

Quantification of mitral cell BDNF-ir was made (see methods) comparing the OB contralateral (open) and ipsilateral (closed) to the occlusion in animals in which deprivation ranged from 20 to 40 days (Figure 2A). We did not observe changes in BDNF-ir labeling intensity of individual mitral cells as a result of the naris occlusion procedure. The number of BDNF-ir mitral cells per unit area, however, was significantly increased at all sampled time points (ANOVA, *Bonferoni's*, $\alpha \leq 0.05$). Interestingly, a similar tabulation for juxtglomerular cells indicated the opposite effect; a significant decrease in BDNF-ir for juxtglomerular cells per unit area at all sampled time points of sensory deprivation (Figure 2B). In a separate set of controls, sham animals (heated probe applied to shank of nose, n = 3) had BDNF-ir profiles (numbers of mitral and juxtglomerular neurons per unit area) that were not different in

numbers per unit area in comparison to that of the contralateral OB (open) from naris-occluded animals following 20 days of treatment (Student's *t*-test, $\alpha \leq 0.05$).

We performed naris occlusion on YFP mice so that BDNF-ir could be followed as a double label with YFP-positive mitral cells. A representative confocal micrograph demonstrating increased mitral cell BDNF-ir per unit area following 30 days sensory deprivation is reported in Figure 3. The secondary dendrites of mitral/tufted cells were restricted to the inner layer of the EPL (EPL) indicating (1) an anatomical subdivision within the EPL and (2) that BDNF-ir fibers in the oEPL do not arise from mitral cells. In a subset of control YFP animals ($n = 3$), we additionally confirmed that absolute numbers of YFP+ mitral cells per unit area were not significantly different following 20 days of sensory deprivation, however, numbers of Dapi-nuclear stained juxtglomerular cells decreased by approximately 20% per unit area (paired *t*-test, $\alpha \leq 0.05$).

Biochemical confirmation of increased expression of mature BDNF at P20 was not evident. In fact, labeling consistent with the mobility of proBDNF ($M_r = 27$ kDa) and a pro-BDNF dimer ($M_r = 54$ kDa) was observed at uniform pixel density independent of the sensory deprivation condition (Figure 4). Since mature BDNF could be detected in control tissue (rat hippocampus, $M_r = 13$ kDa), the level of mature BDNF in the OB may be at or beyond the limits of detection by traditional protein biochemical techniques using this antiserum and our conditions despite our efforts to pool animals, load high concentrations of protein (50 μ g), and incubate with a greater titer of antiserum (1:200).

Discussion

Our study monitors the BDNF-ir profile of OB neurons following unilateral sensory occlusion and demonstrates that the number of immunopositive mitral cells per unit area increases while that of juxtglomerular cells decreases, independent of period of sensory deprivation ranging 20 to 40 days. Decrease in bulb size ipsilateral to the naris closure [22] is attributed mainly to apoptotic cell death in glomerular and granule cell layers, however, the number of mitral cells has been reported to be unaffected [25]. It is possible that sensory deprivation may stimulate mitral cells to synthesize BDNF leading to immunolabeling of cells that would typically escape detection under normal conditions. Because mitral cells have high expression of the *bcl-2* gene that suppresses apoptosis [1,14,17], the susceptibility of mitral cells to apoptotic death could be lower than that for other OB cell-types. It is also known that trophic factors and other survival signals in the developing nervous system may suppress an intrinsic suicide program of cells to regulate cell numbers in response to sensory stimuli [26]. Our correlational biochemistry data may suggest that proBDNF could possibly function as a trophic factor to prevent apoptosis of mitral cells induced by olfactory sensory deprivation. Future experiments would have to be pursued to test this interesting correlation.

Previous studies have revealed that the EPL undergoes the greatest reduction in laminar volume following naris occlusion [22]. Our study using YFP mice may infer that the reduction in EPL thickness following sensory deprivation is due the absence of BDNF-ir fibers in the superficial layer of EPL (oEPL). Although loss of BDNF-ir fibers may not be the sole loss of EPL thickness, genetic deletion of BDNF has been shown to lead to cell and fiber loss in this area of the OB [2]. The origin of the oEPL BDNF-ir fibers described here is not clear, but may belong to secondary dendrites of middle-tufted cells since these dendrites ramify into the superficial EPL [27]. Indeed, Hamilton et al. (2008) have recently shown that middle-tufted cells may undergo trophic changes after adult olfactory-sensory deprivation induced by deafferentation [16]. Our data may, therefore, provide preliminary evidence for a functional segregation within the EPL. Recently Clevenger et al. [6] generated mice in which the BDNF promoter drove expression of β -galactosidase in order to effectively map BDNF transcription

across the bulb and epithelium. Their data suggest a BDNF transcript signal in the EPL that parallels that of our protein level detection by ICC, but curiously they report no transcript detected in mitral cells [6]. Since proBDNF is secreted [3,19,24] and our biochemistry data support the idea that our ICC is labeling pro and not mature BDNF (as discussed below), absence of transcript in the mitral cells would not be inconsistent with our BDNF-ir specific expression patterns. Although there are reported inconsistencies in mitral cell transcription of BDNF [6,9] the majority of studies utilize adult rat, rather than postnatal mice as did our study, and none observed BDNF levels in mice following naris cauterization from birth [21].

The high affinity receptor for mature BDNF, TrkB, is present in various cell types within the rat OB [13] and is predominantly expressed as a full-length receptor [28]. Consequently it was surprising that we did not find a mature form of the receptor's preferred ligand, BDNF, but rather could only resolve the precursor, proBDNF. It is possible that there exists a species difference across rodents, given that biochemical, immunocytochemical and *in situ* hybridization studies have independently revealed the presence of both pro- and mature BDNF in the rat OB [9,21]. Cao et al. [5], however, detect slight amounts of mature BDNF from crude mouse OB extracts, therefore it is likely that the detection limits of mature BDNF by SDS-PAGE in mouse OB has been reached. In fact, the mouse OB has little BDNF (0.5 ng/g wet weight) that could be detected at P30 using an ELISA method [18]. ELISA cannot distinguish between the two forms of BDNF [23], so presumably this quantity represents both forms.

Our Western analysis indicated a minor band of 27 kDa and a major band of 54 kDa representing proBDNF and proBDNF dimer, respectively. The control, rat hippocampus, revealed an additional band at 13 kDa representing mature BDNF and a cluster of high molecular weight bands presumably corresponding to the glycosylated forms of the mature BDNF [24]. Preadsorption of the same antiserum used in our study with BDNF has been shown by Western analysis to quench the proBDNF, but not the mature BDNF, band observed in human cortex [23], which strongly infers that our immunocytochemical signal is proBDNF. If the signal is predominantly proBDNF and not mature BDNF, and two different BDNF-ir cell populations within the bulb are oppositely affected by naris occlusion (mitral cell BDNF-ir is elevated while juxtglomerular cell BDNF-ir is decreased), then it follows that no net change in pixel density of proBDNF might be expected due to a cross-nulling effect.

ProBDNF has been considered an inactive precursor prior to cleavage by the serine protease plasmin and selective matrix metalloproteinases [3,19,24]. The cleaved (mature) BDNF can activate TrkB receptors and promote cell survival and synaptic plasticity. Alternatively, proBDNF may directly bind to and activate TrkB receptors to promote mitral cell survival. In support of this idea, furin-resistant proBDNF, secreted from COS-7 cells, is known to bind to the extracellular domains of both TrkB and p75NTR [11]. Fayard et al. [11] demonstrate that proBDNF binds to and activates TrkB and could be involved in TrkB-mediated neurotrophic activity *in vivo*. In human Alzheimer's disease, a pathological condition of extreme apoptosis, it is quite intriguing that proBDNF levels decrease in the parietal cortex [23].

In summary, our data provide evidence for a neurotrophic role of proBDNF in the mouse olfactory system. Most OB neurons are interneurons that have short life spans and are replaced by neurons migrating from the subventricular zone [29]. ProBDNF may provide the neurotrophic environment necessary for a continuous degenerative/regenerative process inherent in the olfactory system [15]. In fact, BDNF signaling has recently been shown to affect olfactory terminal-arbor pruning under competitive environments [5].

Acknowledgements

We thank Ms. Kimberly Riddle and the Florida State University Department of Biological Science Imaging Resource and both Mr. Robert Daly and Jeffery Godbey who provided excellent mouse colony maintenance. This work was

supported by NIH grants DC03387 and DC00044 from the NIDCD and grants from the FSU Council of Research and Creative Projects (FSU Peg/LEAD).

References

1. Allsopp TE, Wyatt S, Paterson HF, Davies AM. The proto-oncogene *bcl-2* can selectively rescue neurotrophic factor-dependent neurons from apoptosis. *Cell* 1993;73:295–307. [PubMed: 8477446]
2. Berghuis P, Agerman K, Dobszay MB, Minichiello L, Harkany T, Ernfors P. Brain-derived neurotrophic factor selectively regulates dendritogenesis of parvalbumin-containing interneurons in the main olfactory bulb through the PLCgamma pathway. *J Neurobiol* 2006;66:1437–1451. [PubMed: 17013928]
3. Bloom R, Konnerth A. Neurotrophin-mediated rapid signaling in the central nervous system: Mechanisms and functions. *Physiol* 2005;20:70–78.
4. Brunjes PC. Unilateral naris closure and olfactory system development. *Brain Res Rev* 1994;19:146–160. [PubMed: 8167658]
5. Cao L, Dhillia A, Mukai J, Blazeski R, Lodovichi C, Mason CA, Gogos JA. Genetic modulation of BDNF signaling affects the outcome of axonal competition in vivo. *Cur Biol* 2007;17:911–921.
6. Clevenger AC, Salcedo E, Jones KR, Restrepo D. BDNF promoter-mediated β -Galactosidase expression in the olfactory epithelium and bulb. *Chem Senses*. 2008;10.1093/chemse/bjn021
7. Colley BS, Tucker K, Fadool DA. Comparison of modulation of Kv1.3 channel by two receptor tyrosine kinases in olfactory bulb neurons of rodents. *Receptors Channels* 2004;10:25–36. [PubMed: 14769549]
8. Colley BS, Biju KC, Visegrady A, Campbell S, Fadool DA. Neurotrophin B receptor kinase increases Kv subfamily member 1.3 (Kv1.3) ion channel half-life and surface expression. *Neurosci* 2007;144:531–46.
9. Conner JM, Lauterborn JC, Yan Q, Gall CM, Varon S. Distribution of brain-derived neurotrophic factor (BDNF) protein and mRNA in the normal adult rat CNS: evidence for anterograde axonal transport. *J Neurosci* 1997;17:2295–313. [PubMed: 9065491]
10. Cook KK, Fadool DA. Two adaptor proteins differentially modulate the phosphorylation and biophysics of Kv1.3 ion channel by SRC kinase. *J Biol Chem* 2002;277:13268–13280. [PubMed: 11812778]
11. Fayard B, Loeffler S, Weis J, Vögelin E, Krüttgen A. The secreted brain-derived neurotrophic factor precursor pro-BDNF binds to TrkB and p75NTR but not to TrkA or TrkC. *J Neurosci Res* 2005;80:18–28. [PubMed: 15704182]
12. Feng G, Mellor RH, Bernstein M, Keller-Peck C, Nguyen QT, Wallace M, Nerbonne JM, Lichtman JW, Sanes JR. Imaging neuronal subsets in transgenic mice expressing multiple spectral variants of GFP. *Neuron* 2000;28:41–51. [PubMed: 11086982]
13. Fryer RH, Kaplan DR, Feinstein SC, Radeke MJ, Grayson DR, Kromer LF. Developmental and mature expression of full-length and truncated TrkB receptors in the rat forebrain. *J Comp Neurol* 1996;374:21–40. [PubMed: 8891944]
14. Garcia I, Martinou I, Tsujimoto Y, Martinou JC. Prevention of programmed cell death of sympathetic neurons by the *bcl-2* proto-oncogene. *Science* 1992;258:302–304. [PubMed: 1411528]
15. Graziadei PP, Monti Graziadei GA. Neurogenesis and plasticity of the olfactory sensory neurons. *Ann NY Acad Sci* 1985;457:127–142. [PubMed: 3913359]
16. Hamilton KA, Parrish-Aungst S, Margolis FL, Erdelyi F, Szabo G, Puche AC. Sensory deafferentation transsynaptically alters neuronal GluR1 expression in the main olfactory bulb. *Chem Senses* 2008;33:201–10. [PubMed: 18184638]
17. Hockenbery DM, Oltvai ZN, Yin XM, Milliman CL, Korsmeyer SJ. Bcl-2 functions in an antioxidant pathway to prevent apoptosis. *Cell* 1993;75:241–251. [PubMed: 7503812]
18. Kato-Semba R, Semba R, Takeuchi IK, Kato K. Age-related changes in level of brain-derived neurotrophic factor in selected brain regions of rats, normal mice and senescence-accelerated mice: A comparison to those of nerve growth factor and neurotrophin-3. *Neuroscience Res* 1998;31:227–234.

19. Lee R, Kermani P, Teng KK, Hempstead BL. Regulation of cell survival by secreted proneurotrophins. *Science* 2001;294:1945–1948. [PubMed: 11729324]
20. Marks DR, Fadool DA. Post-synaptic density perturbs insulin-induced Kv1.3 channel modulation via a clustering mechanism involving the SH(3) domain. *J Neurochem* 2007;103:1608–1627. [PubMed: 17854350]
21. McLean JH, Darby-King A, Bonnell WS. Neonatal olfactory sensory deprivation decreases BDNF in the olfactory bulb of the rat. *Brain Res Dev Brain Res* 2001;128:17–24.
22. Meisami E. Effects of olfactory deprivation on postnatal growth of the rat olfactory bulb utilizing a new method for production of neonatal unilateral anosmia. *Brain Res* 1976;107:437–444. [PubMed: 1268738]
23. Michalski B, Fahnstock M. Pro-brain-derived neurotrophic factor is decreased in parietal cortex in Alzheimer's disease. *Mol Brain Res* 2003;111:148–154. [PubMed: 12654514]
24. Mowala SJ, Farhadi HF, Pareek S, Atwal JK, Morris SJ, Seidah NG, Murphy RA. Biosynthesis and post-translational processing of the precursor to brain-derived neurotrophic factor. *J Biol Chem* 2001;276:12660–12666. [PubMed: 11152678]
25. Najbauer J, Leon M. Olfactory experience modulated apoptosis in the developing olfactory bulb. *Brain Res* 1995;674:245–251. [PubMed: 7796103]
26. Raft MC, Barres BA, Burne JF, Coles HS, Ishizaki Y, Jacobson MD. Programmed cell death and the control of cell survival: lessons from the nervous system. *Science* 1993;262:695–700. [PubMed: 8235590]
27. Shepherd, GM.; Greer, CA. Olfactory bulb. In: Shepherd, GM., editor. *The synaptic organization of the brain*. 4. Oxford University Press; Oxford: 1998. p. 159-204.
28. Tucker K, Fadool DA. Neurotrophin modulation of voltage-gated potassium channels in rat through TrkB receptors is time and sensory experience dependent. *J Physiol* 2002;542:413–29. [PubMed: 12122142]
29. Whitman MC, Greer CA. Synaptic integration of adult-generated olfactory bulb granule cells: basal axodendritic centrifugal input precedes apical dendrodendritic local circuits. *J Neurosci* 2007;27:9951–61. [PubMed: 17855609]

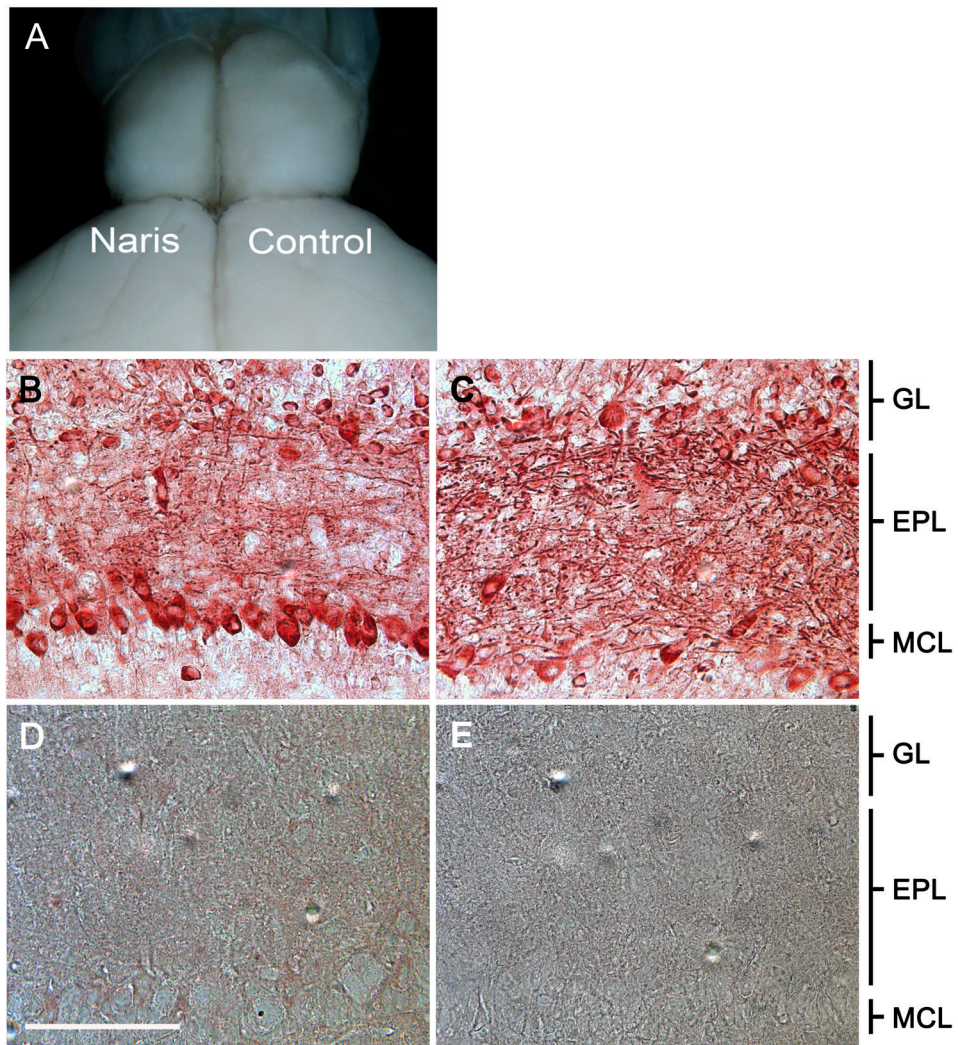


Figure 1.

Unilateral-naris occlusion induces anatomical changes in the mouse olfactory bulb. (A) This representative mouse was naris occluded within 24 hours of birth and photographed on postnatal day twenty (P20). Olfactory bulb (OB) ipsilateral to the occluded nostril (Naris) versus that of the contralateral control (Control). Representative photomicrographs at P20 comparing BDNF immunoreactivity (BDNF-ir) in the (B) olfactory bulb ipsilateral to the naris occlusion and the (C) control olfactory bulb. (D) Preadsorption control with rhBDNF. (E) No primary control. EPL, external plexiform layer; GL, glomerular layer; MCL, mitral cell layer. Scale bar, 100 μm .

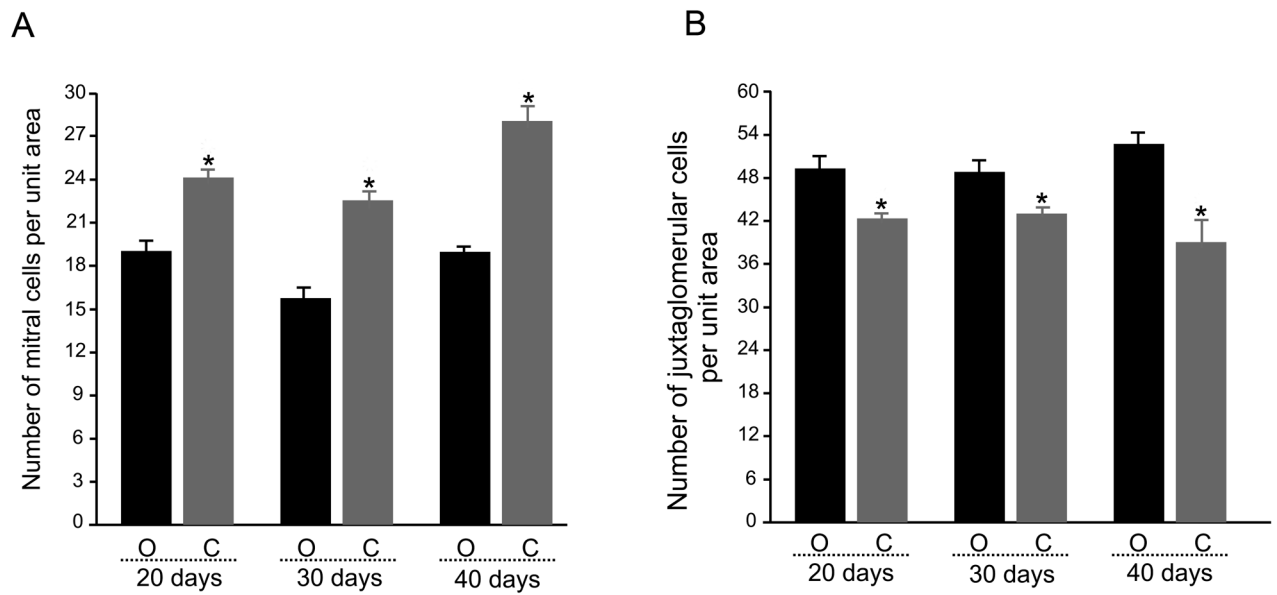


Figure 2.

Bar plot of the mean number (per $93,500 \mu\text{m}^2$) of (A) mitral cells and (B) juxtglomerular cells in a population of OBs contralateral to the naris-occlusion (O, open) versus that for OBs ipsilateral to the naris-occlusion (C, closed). Data represent mean \pm standard error of the mean for three sections analyzed across quadrants (dorsal, ventral, medial, lateral) acquired from 15 animals in each of three occlusion durations. * = Significantly-different by mixed-block factorial design ANOVA, *Bonferoni's*, $\alpha \leq 0.05$.

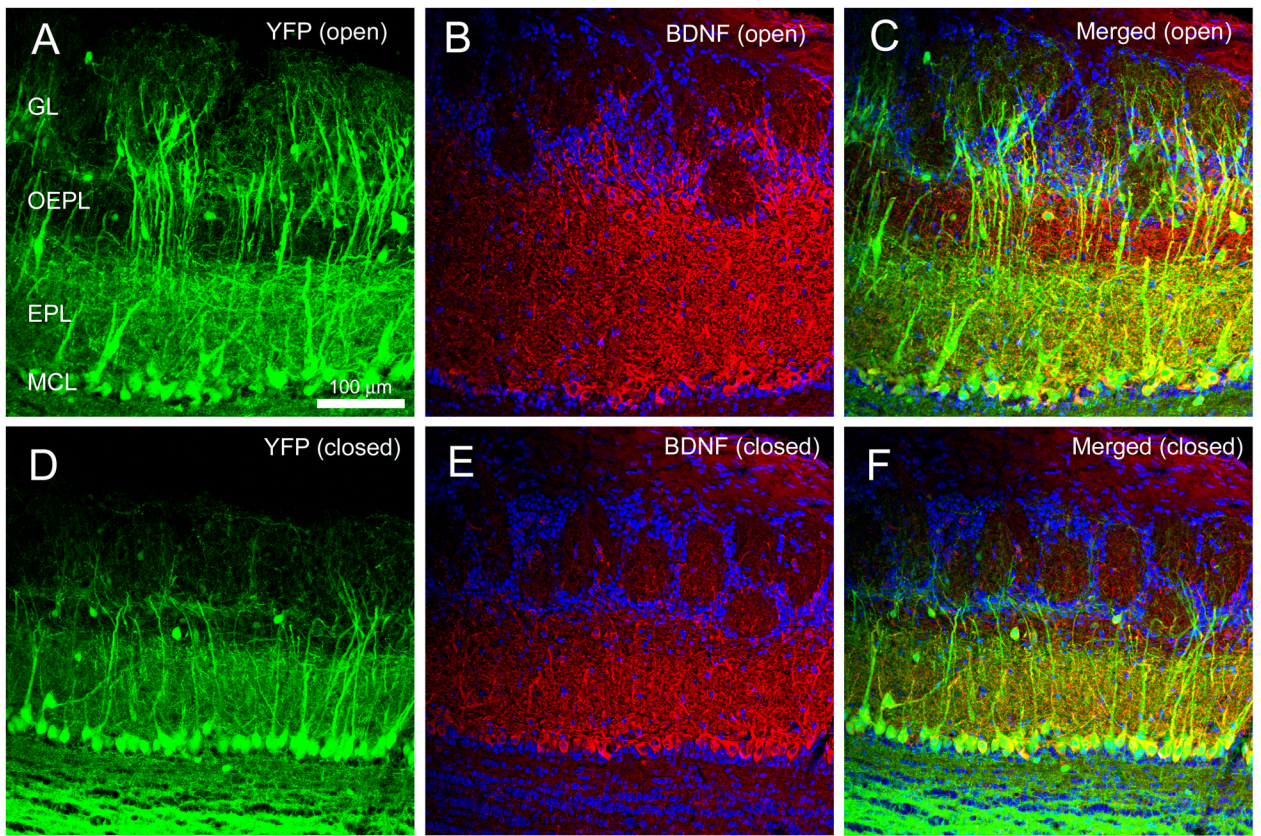


Figure 3. Representative double-color BDNF immunocytochemistry of the olfactory bulb of *thy1* YFP transgenic mice (YFP) following 30 days of sensory deprivation as imaged on a confocal system. (A) Contralateral control OB (YFP (open)). (B) Same, but demonstrating BDNF-ir (BDNF (open)), and (C) merged image. (D–F) Same as (A–C) but for the OB ipsilateral to the naris occlusion. EPL, external plexiform layer; GL, glomerular layer; MCL, mitral cell layer; Scale bar, 100 μm.

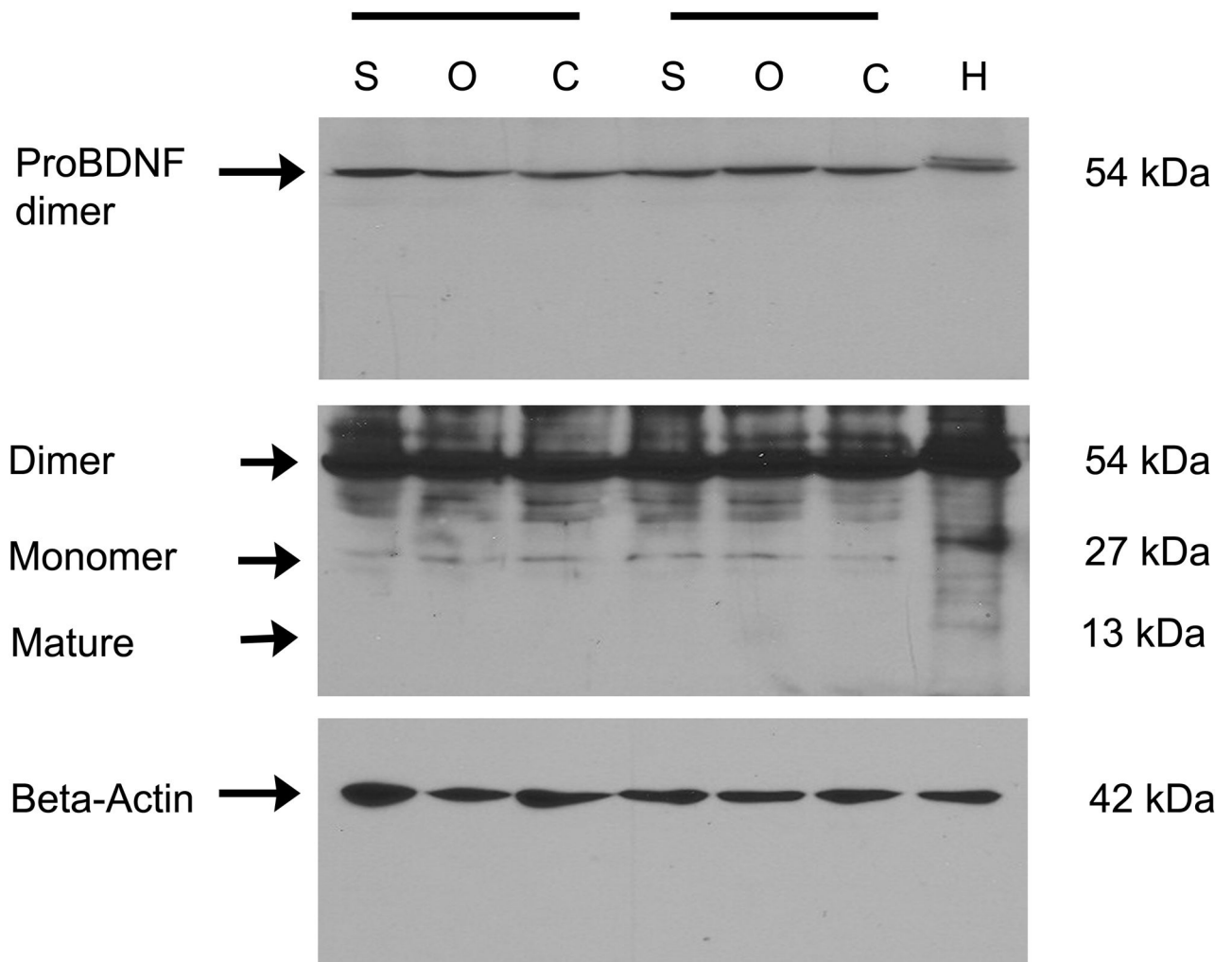


Figure 4. Confirmation of antiserum specificity by Western blot analysis. Shown are detergent-solubilized (NP-40) protein fractions electrophoretically separated using 15% SDS PAGE. Two representative trial blocks are shown (horizontal bars) for sham treatment (S), contralateral control OB (O, open), and ipsilateral naris-occluded OB (C, closed). H, rat hippocampus. Top blot: proBDNF dimer is observed following a short exposure (30 s) of the film. Middle blot: Same blot, but a longer exposure (5 min) was used to visualize the proBDNF monomer (Monomer) and mature BDNF (Mature). Bottom blot: Nitrocellulose was stripped and reprobed for beta-actin to demonstrate equal protein loading across treatments.